Multilevel autoregulation of λ repressor protein CI by DNA looping in vitro

Dale Lewis[a], Phuoc Le[a], Chiara Zurla[b], Laura Finzi[c], and Sankar Adhya[a,1]

[a]Laboratory of Molecular Biology, Center for Cancer Research, National Cancer Institute, National Institutes of Health, Bethesda, MD 20892-4264; [b]Department of Biomedical Engineering, Georgia Institute of Technology, Atlanta, GA 30332; and [c]Physics Department, 400 Dowman Drive, Emory University, Atlanta, GA 30322

Contributed by Sankar Adhya, July 15, 2011 (sent for review January 28, 2011)

The prophage state of bacteriophage λ is extremely stable and is maintained by a highly regulated level of λ repressor protein, CI, which represses lytic functions. CI regulates its own synthesis in a lysogen by activating and repressing its promoter, P_{RM}. CI participates in long-range interactions involving two regions of widely separated operator sites by generating a loop in the intervening DNA. We investigated the roles of each individual site under conditions that permitted DNA loop formation by using in vitro transcription assays for the first time on supercoiled DNA that mimics in vivo situation. We confirmed that DNA loops generated by oligomerization of CI bound to its operators influence the autoactivation and autorepression of P_{RM} regulation. We additionally report that different configurations of DNA loops are central to this regulation—one configuration further enhances autoactivation and another is essential for autorepression of P_{RM}.

activation | cooperativity | repression

Bacteriophage lambda (λ) of *Escherichia coli* can grow either in a lytic or lysogenic mode. In a lysogenic cell, the phage-encoded λ repressor protein (CI) prevents lytic growth by directly repressing two promoters needed to express lytic functions, P_L and P_R (1–3). Each promoter is associated with a CI recognition site or operator, O_L (composed of three adjacent subsites, O_L1, O_L2, O_L3) and O_R (O_R1, O_R2, O_R3). O_R is associated with promoter P_{RM} (promoter for maintenance of repressor synthesis), which directs transcription of the *cI* gene in the prophage state (4–6). Each subsite binds a CI dimer (7).

The CI protein autoregulates its synthesis. At low cellular CI concentration, CI enhances its own synthesis from P_{RM}; when high, CI represses P_{RM} (1, 8, 9). It was originally believed that both positive and negative autoregulations are achieved exclusively by the action of CI dimers at the P_{RM}-O_R-P_R sequence of the phage genome (1, 10) (Fig. 1*A*), based on the following observations. (*i*) There is a hierarchy of intrinsic binding affinities of a CI dimer to individual operators sites: $O_R1 > O_R2 > O_R3$ (11–17); (*ii*) CI bound to the intrinsically weak O_R2 site is strengthened by cooperative interactions with CI bound to the stronger adjacent O_R1 site, and the ensemble of two CI dimers at the $O_R1 \sim O_R2$ sites represses P_R and activates P_{RM} (13, 16) (Fig. 1*A*); (*iii*) at high CI concentrations, a CI dimer can bind to the weakest operator site, O_R3, repressing P_{RM} (1, 2) (Fig. 1*C*). Incidentally, a second pair of CI dimers binds cooperatively to $O_L1 \sim O_L2$, and represses P_L (7).

This model was recently modified on the basis of physical and genetic experiments showing that a CI tetramer cooperatively bound to $O_R1 \sim O_R2$ interacts with a tetramer cooperatively bound to $O_L1 \sim O_L2$, located 2.3 kbp away (18–21), resulting in the looping out of the intervening DNA, as shown by electron and atomic force microscopy (18, 22, 23). DNA loop was also observed by cooperative interactions of CI at sites separated by only five and six helical turns (23, 24). The kinetic and thermodynamic properties of loop formation were determined by single DNA molecule analysis (25, 26). Mathematical modeling and genetic studies suggested that DNA looping further enhances

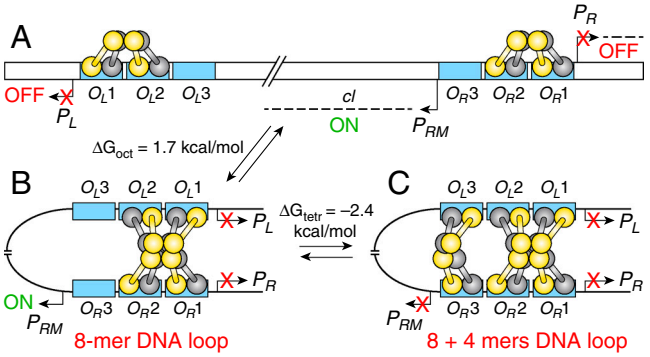

Fig. 1. Models of CI regulation by DNA looping. Detailed conformations of the structures are not known and maps are not drawn to scale. (*A*) Promoters (P_R, P_L, and P_{RM}); operators O_L (O_L1, O_L2, O_L3) and O_R (O_R1, O_R2, O_R3) are in blue rectangles; CI dimers (one monomer is shown in yellow, the other is in gray). The bent arrows show the transcription start points of promoters. The dashed line indicates transcripts from P_R, P_L, and P_{RM}. The *cI* gene is transcribed from P_{RM}. (*B*) DNA looping and octamer formation (8-mer) by CI tetramer binding to $O_L1 \sim O_L2$ interacts with that at $O_R1 \sim O_R2$. (*C*) Octamer and tetramer (12-mer) of CI binding to O_L and O_R. Red X means promoter is turned off. ΔG_{oct} and ΔG_{tetr} values for octamer and tetramer loops stability are from Zurla et al. (25), measured on linear DNA under different conditions. See refs. 7, 18, 20, and 59 for models on CI regulation.

autoactivation of P_{RM} (27, 28). Genetic experiments also indicated that $O_R1 \sim O_R2/O_L1 \sim O_L2$ mediated DNA looping helps CI autorepression by stabilizing CI dimer binding at O_R3 through a cooperative interaction with a CI dimer bound to O_L3 (19, 20) (Fig. 1*C*).

We previously investigated the thermodynamic parameters of DNA loops with or without the involvement of O_L3 and O_R3 by tethered particle microscopy of single DNA molecules (25). The results showed that, whereas the DNA loops, which involve all six operators and six CI dimers are relatively stable (Fig. 1*C*), those without O_R3 and O_L3 and involving only four dimers are less stable (Fig. 1*B*). However, the stabilities were determined on linear DNA compared to the transcription experiments (see below) performed using supercoiled DNA templates. These studies cannot provide insight into the properties of the P_{RM} promoter itself. The original model of P_{RM} regulation by CI was based on studies using DNA templates carrying the O_R region only (1–3, 7). To study the involvement of O_L in the regulation of P_{RM}, we reasoned that the weak interaction forming the octamer might not allow us to detect activation caused by looping using linear templates. Because it is believed that supercoiling increases

Author contributions: D.L., L.F., and S.A. designed research; D.L., P.L., and C.Z. performed research; P.L. and C.Z. contributed new reagents/analytic tools; D.L., L.F., and S.A. analyzed data; and D.L. and S.A. wrote the paper.

The authors declare no conflict of interest.

[1]To whom correspondence should be addressed. E-mail: adhyas@mail.nih.gov.

This article contains supporting information online at www.pnas.org/lookup/suppl/doi:10.1073/pnas.1111221108/-/DCSupplemental.

the local concentration of distant sites (29), we chose to use supercoiled templates in a transcription assay to more closely reflect the in vivo situation. Thus, we developed an in vitro transcription system using supercoiled templates. With this system, we have confirmed in vitro the enhancement of P_{RM} autoactivation by the less stable DNA loop mediated by four CI dimers, which forms at physiological concentrations of CI. The physiological concentration of monomeric CI in a lysogenic cell is 200 nM (6, 17, 30, 31). We confirmed the cooperative role of O_L3 and O_R3 in P_{RM} repression. Additionally, we also discuss that it is the difference in loop configuration that modulates activation or promotes repression.

Results

We used our in vitro transcription system containing supercoiled DNA templates with the prophage promoters P_R, P_L, and P_{RM} to investigate the autoregulation of CI by DNA looping. We designed and constructed the templates in order to produce in the same assay the following discrete RNA sizes: P_R, 117 nt; P_L, 167 nt; and P_{RM}, 212 nt (Fig. 2*A*). The distance between the midpoint of O_L3 and O_R3 is 392 bp in most DNA templates with an integration host factor (IHF) binding site and an "up" element between O_L3 and the T_{imm} terminator (Fig. 2*A*). The in vitro transcription results from the phage promoters in the presence of increasing concentrations of total CI monomers in a supercoiled DNA template (pDL944) with wild-type operators as shown in Fig. 2 *B* and *C*. As expected, CI efficiently repressed the lytic promoters, P_L and P_R; half-maximal repression (0.5-fold) of P_L and P_R occurred at 50 nM CI. P_{RM} was maximally activated (more than ninefold) at 80 nM CI; transcription from P_{RM} was repressed at higher CI concentrations (Fig. 2 *B* and *C*). Half-maximal activation and repression of P_{RM} occurred at 50 and 320 nM CI, respectively. The observed regulatory pattern was qualitatively similar to previous in vitro and in vivo results, where P_{RM} was maximally stimulated 10-fold with respect to its basal level (1, 2, 8).

The intrinsic promoter strength of P_{RM} was very low in the pDL944 template (Fig. 2*B*, lane 1). To increase the sensitivity of P_{RM} in our assays, we used an "up mutation" (*prmup*-1, henceforth called $P_{RM}1$), which changes the −35 element of P_{RM} from $^{-35}$TAGATA^{-30} to $^{-35}$TAGACA^{-30} at position −31, creating plasmid pDL985 (1, 16). The increase in the basal activity of $P_{RM}1$ relative to P_{RM} without CI was sevenfold (Fig. 3*A*, lane 1). At 160 nM CI, $P_{RM}1$ was maximally stimulated threefold, which is in agreement with three- and fourfold activation of $P_{RM}1$ in vivo (1, 2, 16, 32, 33) (Fig. 3 *A* and *C*). Half-maximal activation and repression occurred at 60 and 500 nM CI, respectively. At very high concentrations of CI, $P_{RM}1$ was repressed below its basal level (lanes 11–12). Thus, the regulatory effect of CI on the transcripts of $P_{RM}1$ was as in the WT P_{RM} template except that P_{RM} was activated 10-fold, whereas $P_{RM}1$ was activated threefold (Figs. 2 and 3). Both promoters were repressed at high CI concentrations.

The WT distance between O_L3 and O_R3 is 2.3 kbp. To substantiate the results described above and correlate them to WT DNA length, we tested a $P_{RM}1$ template, pDL1133, containing the natural length of 2.3 kbp between O_L3 and O_R3 (with *rex*B, *rex*A, IHF site, and up element) (Fig. S1 *A* and *B*). We inserted an additional transcription terminator (*rpo*C$_{ter}$) downstream of $P_{RM}1$ in the *cI* gene to reduce the size of $P_{RM}1$ transcript to 96-nt from its natural length of approximately 2,136 nt, which would have been difficult to detect in our RNA gels (Fig. S1 *A*). $P_{RM}1$ was activated 3.5-fold at 80 nM CI before being repressed at higher CI concentrations (Fig. 3 *B* and *C*). Half-maximal activation and repression occurred at 40 and 350 nM CI, respectively. Above 600 nM of CI, $P_{RM}1$ was repressed below its basal level of expression. The decrease in $O_L \sim O_R$ spacing did not significantly change P_{RM} autoregulation. In the other experiments, we studied P_{RM} regulation using $P_{RM}1$ DNA templates with a 392-bp separation between O_L3 and O_R3. We believe that the use of $P_{RM}1$ and shortened $O_L \sim O_R$ distance in the DNA template would not hinder our goals of studying P_{RM} regulation. We also assumed that an "antiparallel" loop, and not a "parallel" loop, is the preferred loop geometry (34, 35). Though there is a possibility that with longer operator spacing, there might be some form of parallel loops, previous data show that a short distance favors the antiparallel orientation in a DNA loop (34, 35).

Effect of Each Operator on $P_{RM}1$ Regulation. To investigate the role of each of the six operators in $P_{RM}1$ regulation, we inactivated each operator by changing the conserved ^{4}CACCG^{8} to ^{4}CAATG^{8} sequence in the consensus half-site to remove the operator recognition for CI (Fig. 4*A*) (36). This 2-bp sequence is important for CI binding as determined by genetic studies (1).

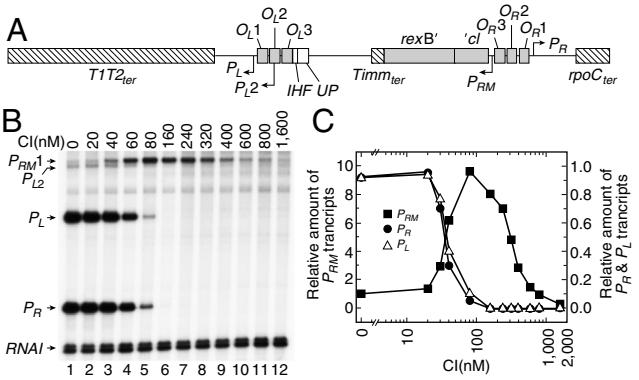

Fig. 2. Regulation of P_R, P_L, P_{L2}, and P_{RM} by CI. (*A*) Map is drawn to scale with the O_L and O_R regions in black rectangles, promoters (P_R, P_L, P_{L2}, and P_{RM}). The hatched boxes show the terminators ($T1T2_{ter}$, $Timm_{ter}$, and *rpoC*$_{ter}$). An IHF binding site and an "up element" are located to the right of O_L3 (42, 43). Partial *rex*B and *cI* genes are shown upstream of P_{RM}. The distance between the centers of O_L3 and O_R3 is 392 bp. (*B*) RNAs made from wild-type plasmid in *A* with increasing total CI monomer concentrations (nanomolar). *RNA*I transcripts are control RNAs. P_{L2}, a minor promoter with its transcription start point located 42-bp upstream of that of P_L, was also repressed by CI (42, 43). The physiological significance of P_{L2} is not known. (*C*) Quantification of the transcripts in *B*. The P_R, P_L, and P_{RM} transcripts are normalized to *RNA*I and to the amount of transcripts in the absence of CI (lane 1) for each promoter. Therefore, the amount of each transcript made in lane 1 is taken as 1.0. The relative amount of transcripts (*y* axis) is plotted against the total CI monomer concentration (*x* axis). The *x* axis has a break from 3–4 nM CI and a log scale after the break.

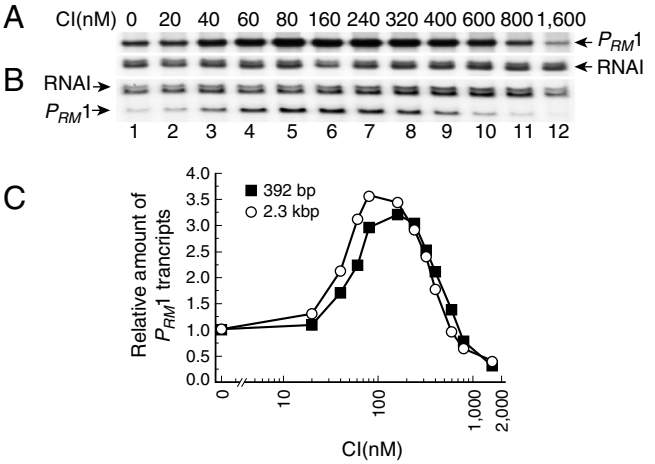

Fig. 3. Effect of DNA spacer length on $P_{RM}1$ regulation. (*A*) RNAs made from $P_{RM}1$ plasmid (392-bp spacer). (*B*) RNAs from $P_{RM}1$ with 2.3-kbp spacer. (*C*) Quantification of RNAs from $P_{RM}1$ with 392-bp (*A*) and 2.3-kbp spacers (*B*).

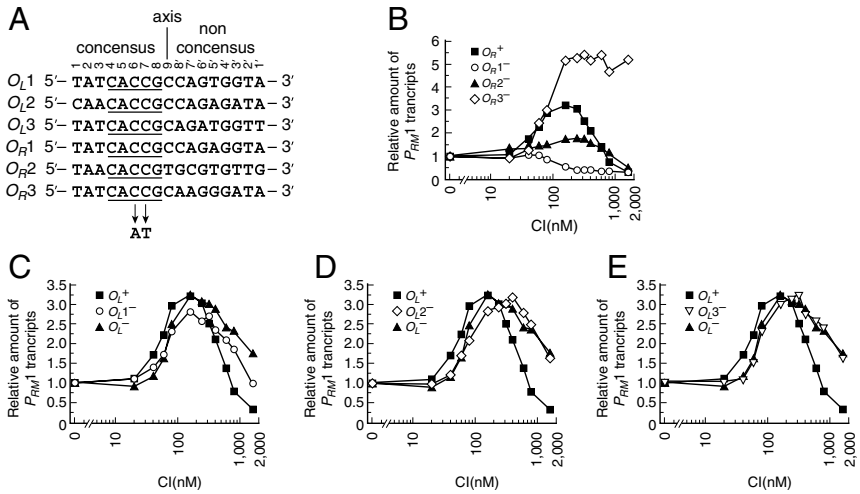

Fig. 4. Effect of operator mutations on $P_{RM}1$ regulation. (*A*) Alignment of operators' sequences showing the consensus (1–8) and nonconsensus (1′–8′) half-sites. The axis of symmetry passes through the ninth base pair. The conserved penta site (CACCG) is underlined. A change of CC to AT inactivates each operator site. (*B*) Quantification of $P_{RM}1$ RNAs made from templates containing O_R operators (Fig. S3 *A–D*). (*C–E*) Quantification of $P_{RM}1$ RNAs made from templates with mutations in O_L operators (Fig. S3 *E–H*). The data for the O_L^+ and O_L^- constructs are shown in panels *C–E*, which are separated for clarity.

Structural studies showed that Lys-4 and Asn-55 of CI contact the G residues at positions -6CG and -7CG of O_R1 or O_L1 (12, 37–40). Both bases are important for CI recognition because changing of either base resulted in a large positive value of ΔG (12, 38, 39). Such mutations in all six operators at the same time prevented both activation of $P_{RM}1$ and repression of P_R and P_L by CI, confirming that the mutant operators are nonfunctional (Fig. S2).

First, we studied the contribution of individual $O_R$operator elements in $P_{RM}1$ regulation by CI on templates containing O_L^+ operators.

(*i*) Mutation in O_R1 is expected to stabilize a CI dimer at weak O_R3 because of a cooperative interaction with CI bound at O_R2 even at low concentrations, which increases the affinity of O_R3 by fivefold (16, 31). Such binding should prevent activation and enhance repression of P_{RM}. In agreement, we found that inactivation of O_R1 resulted in repression of $P_{RM}1$ even at 80 nM of CI and no activation at any CI concentrations (Fig. 4*B* and Fig. S3*B*). We propose that this strong repression of $P_{RM}1$ was due to both $O_R2 \sim O_R3$ cooperativity and the interactions of the CI tetramers at $O_R2 \sim O_R3$ and $O_L1 \sim O_L2$ by a shift of CI partners changing to a different register because in an $O_L^- O_R1^-$ template, $P_{RM}1$ repression occurred at higher CI concentrations relative to $P_{RM}1$ repression in an $O_L^+O_R1^-$ template (Fig. S4).

(*ii*) Because O_R3 is only involved in P_{RM} repression, mutation in O_R3 is not expected to affect the activation of P_{RM}. Indeed, the $P_{RM}1$ activity was stimulated to a maximum level of fivefold at 160 nM CI in the O_R3 mutant template and no repression was observed at higher CI concentrations as expected (Fig. 4*B* and Fig. S3*C*).

(*iii*) We expected that mutation of O_R2 would eliminate $P_{RM}1$ activation, but we observed a small amount of $P_{RM}1$ activation (1.7-fold) in the O_R2^- template at 240 nM CI before the repression brought about by O_R3 occupation at higher CI concentrations (Fig. 4*B* and Fig. S3 *A* and *D*). Meyer et al. also showed a low level of P_{RM} activation (*ca.* twofold) in O_R2^- mutants (*vir*C23 and *v*1) (1, 10). They suggested that this low level of activation was due to CI binding to O_R1 because, in an O_R1 mutant, the activation was eliminated. We propose that this activation may be due to some level of CI binding to the defective O_R2 site because of cooperative interactions with a dimer bound at O_R1 at high CI concentrations, as suggested previously (41) to explain the rescue of CI binding to a mutated O_R3 site. Incidentally, we also investigated whether the observed $P_{RM}1$ repression in the O_R2^- template is because of a DNA loop formed by a cooperative interaction between CI bound to O_R1 and O_R2^- that aids an interaction between CI at O_L3 and O_R3. A DNA loop is involved in $P_{RM}1$ repression because the repression was eliminated in the $O_L^-O_R2^-$ double mutant (Fig. S5).

The above experiments performed in the presence of the O_L region and, therefore, under conditions that permitted DNA looping could assist CI binding at O_R3 to elicit $P_{RM}1$ repression at lower CI concentrations than in the absence of O_L. To confirm the role of the O_L region and DNA looping in the regulation of $P_{RM}1$, we first tested a template in which all three O_L elements were mutated (triple mutant, O_L^-) to eliminate DNA looping. In contrast to the wild-type ($O_L^+O_R^+$) template where half-maximal repression of $P_{RM}1$ occurred at 500 nM CI, complete repression of $P_{RM}1$ in $O_L^-O_R^+$ did not occur even at 800 nM CI (Fig. 4*C* and Fig. S3*E*). At this CI concentration, $P_{RM}1$ was repressed in $O_L^+O_R^+$ relative to $O_L^-O_R^+$ by threefold and this difference increased to fivefold at 1,600 nM CI. This weak repression of $P_{RM}1$ in $O_L^-O_R^+$ probably reflects the low intrinsic binding of CI to O_R3 in the absence of DNA looping (Fig. 4*C* and Fig. S3*E*). In $O_L^+O_R^+$, $P_{RM}1$ was repressed below its basal level at high CI concentrations, whereas in $O_L^-O_R^+$, $P_{RM}1$ repression level was above the basal level. In addition, O_L^+ needed less CI than O_L^- for activation, suggesting that DNA looping enhances activation. This activation became evident when O_R3 was mutated to eliminate the repression of $P_{RM}1$ (see below). These results confirm that DNA looping enhances P_{RM} activation and is essential for P_{RM} repression at just above physiological CI concentrations.

Next, we assayed the contribution of individual O_L operator elements in $P_{RM}1$ regulation by CI on templates containing O_R^+ operators.

(*i*) Mutation in O_L1 reduced activation and repression of $P_{RM}1$ with respect to the WT operator (Figs. 4*C* and Fig. S3*F*). Half-maximal activation of $P_{RM}1$ occurred at 60 nM CI, and full $P_{RM}1$ repression did not occur even at 800 nM CI. To explain this result, we suggest that mutation in O_L1 allows the CI tetramer at $O_L2 \sim O_L3$ to interact cooperatively with a CI tetramer at $O_R1 \sim O_R2$ by shifting the register, forming an octamer that mediates DNA looping (Fig. S3*F*). The $O_L2 \sim O_L3/O_R1 \sim O_R2$ loop configuration slightly reduced the activation level of $P_{RM}1$ by an unknown mechanism compared to the $O_L1 \sim O_L2/O_R1 \sim O_R2$ loop configuration. In the former configuration, CI at O_L3 is not available to stabilize a CI dimer at O_R3. Therefore, above physiological monomeric CI concentration of 200 nM, $P_{RM}1$

should be activated but not repressed fully. Although half-maximal activation of $P_{RM}1$ occurred at the same concentration (60 nM) as with the WT template, the maximum stimulatory effect of CI was reduced (Fig. 4*C*). We infer that the $O_L2 \sim O_L3/O_R1 \sim O_R2$ loop configuration cannot support full activation; the mechanistic basis for this effect remains to be investigated.

(*ii*) In an O_L2 mutant, $P_{RM}1$ repression was reduced to the same level observed in O_L^-, suggesting that O_L2 is also needed for normal $P_{RM}1$ repression (Figs. 4*D* and Fig. S3*G*). Half-maximal activation of $P_{RM}1$ occurred at 80 nM CI like O_L1^-, and 1,600 nM CI was unable to repress $P_{RM}1$ completely. In the absence of CI binding at O_L2, we expected that the octameric loop complex of CI between $O_R1 \sim O_R2$ and $O_L1 \sim O_L2$ would not form and the cooperative interaction between CI dimers bound to O_L3 and O_R3 would be less efficient or ineffective.

(*iii*) In the O_L3 mutant like O_L2^- and O_L^-, repression of $P_{RM}1$ at 800 and 1,600 nM CI was three- and fivefold weaker than in WT O_L^+, respectively. Half-maximal activation of $P_{RM}1$ occurred at 80 nM as in O_L^-. Why there is no activation enhancement of an $O_L1 \sim O_L2$ and $O_R1 \sim O_R2$ mediated octameric loop on O_L3^- template is unknown. We propose that, in the absence of a stabilizing interaction due to CI binding to O_L3, O_R3 occupancy by CI occurs only at very high CI concentrations due to poor intrinsic affinity and no cooperative effect with O_L3 (Fig. 4*E* and Fig. S3*H*). The O_L2 operator is essential for octamer-mediated loop formation, which juxtaposes a CI bound to O_L3 with a CI bound to O_R3 in the antiparallel loop orientation. Our results also suggest that formation of an octameric loop by itself does not lead to P_{RM} repression; an intact O_L3 must be available for interaction between CI at O_L3 and O_R3 as was interpreted from previous genetic experiments (20). These results confirm that efficient P_{RM} autorepression at physiological concentrations by CI requires DNA looping with a tetramer of CI between O_L3 and O_R3 plus the octamer of CI between $O_L1 \sim O_L2$ and $O_R1 \sim O_R2$ (20).

Finally, in order to investigate the contribution of looping to $P_{RM}1$ activation, we compared the effect of increasing CI concentrations on transcription from $O_L^-O_R3^-$ and $O_L3^-O_R3^-$ templates (Fig. 5 and Fig. S3 *I* and *J*). In such templates, $P_{RM}1$ activation is no longer obscured by the repression mediated by CI bound to O_R3, and in the $O_L^-O_R3^-$ template, no looping occurs (Fig. S3*I*). The O_R3 mutation is used to prevent any $P_{RM}1$ repression, thereby allowing activation to occur at its maximum level. We found that, at high CI concentrations, $P_{RM}1$ was activated up to a maximum of fivefold in the $O_L^-O_R3^-$ template (nonlooping) and eightfold in the $O_L3^-O_R3^-$ template (looping), (Fig. 5 and Fig. S3 *I* and *J*). We argue that this 1.6-fold increase in $P_{RM}1$ activation in the O_L3^- compared to O_L^- template is caused by formation of an octamer among repressor dimers bound to $O_R1 \sim O_R2$ and $O_L1 \sim O_L2$. It was previously shown in vivo that DNA looping can enhance P_{RM} activation from two- to fourfold (27, 28). Recent in vivo reporter assays on *prm*240, a down-promoter mutation of P_{RM}, template showed that DNA looping can enhance P_{RM} activation by fivefold (41). It has been proposed that the stimulating effect of DNA looping on the activation of P_{RM} transcription is attributable to a sterically feasible interaction between the α-carboxyl terminal domain (α-CTD) of RNA polymerase at P_{RM} and an up element located immediately rightward of O_L3 (42, 43). Due to an antiparallel loop configuration, the up element is brought into proximity to contact the α-CTD.

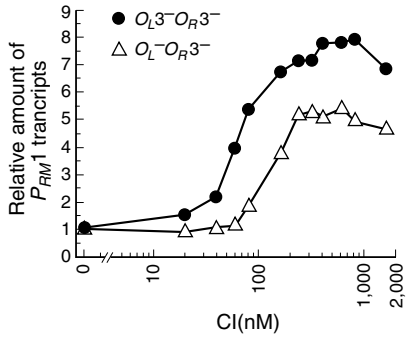

Fig. 5. Stimulatory effect of DNA looping on $P_{RM}1$ expression. Quantification of $P_{RM}1$ RNAs made from looping ($O_L3^-O_R3^-$) and nonlooping ($O_L^-O_R3^-$) templates (Fig. S2 *I* and *J*).

Role of Cooperative Binding in Autoactivation. To determine the contribution of CI bound at O_R2 on $P_{RM}1$ autoactivation in the absence of other regulatory influences, and we used an $O_L^-O_R3^-1^-$ template, which should eliminate the effects of DNA looping, autorepression, and CI cooperative binding to$O_R1 \sim O_R2$. In the presence of the O_R2 operator only, half-maximal activation of $P_{RM}1$ occurred at 600 nM CI, which was 10-fold higher than 60 nM CI required for half-maximal activation of $P_{RM}1$ on WT operator template (Fig. 6 and Fig. S3*K*). No $P_{RM}1$ repression was seen, as expected from the absence of CI binding to O_R3. The absence of cooperativity can explain the higher CI concentration required for $P_{RM}1$ activation and reflects the contribution of only O_R2 in $P_{RM}1$ activation of CI without any cooperative binding.

To confirm that enhancement of activation at physiological CI level is due to cooperative CI binding, we tested the effect on $P_{RM}1$ transcription of two noncooperative CI protein mutants (G147D and D197G; refs. 44–47) using a WT template. Both CI mutants bind to the operators as dimers and are defective in adjacent and distal cooperative interactions between CI dimers (46, 48–51). The crystal structure of the CI D197G: O_L1 complex revealed important information about cooperative binding to adjacent sites (52). Half-maximal activation of $P_{RM}1$ in G147D and D197G were observed at 400 and 350 nM mutant CI, respectively (Fig. 6 and Fig. S3 *L* and *M*). $P_{RM}1$ repression was not observed in the presence of G147D and D197G proteins, but the observed $P_{RM}1$ activation corresponds to a CI dimer bound to O_R2 in the absence of adjacent mutant operators. As expected, in the absence of cooperative binding to adjacent and distal sites, only the intrinsic binding of CI to O_R2 contributed to the low level of activation. In the absence of cooperativity between mutant CI dimers, the O_L3 and O_R3 repression of $P_{RM}1$ at lower CI concentrations did not occur. The two approaches (CI mutants in WT operator and WT CI in $O_L^-O_R3^-1^-$ mutant operator yielded highly consistent results with one another and allowed quantification of the contribution of O_R2 alone in $P_{RM}1$ activation.

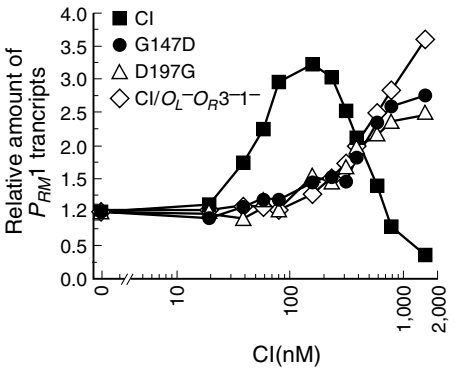

Fig. 6. Effect of CI binding to O_R2 on $P_{RM}1$ expression. Quantification of $P_{RM}1$ RNAs made from control DNA ($O_L^+O_R^+$) in the presence of WT CI and mutant CI (G147D) and (D197G). RNAs from $O_L^-O_R3^-1^-$ DNA in the presence of WT CI (Fig. S2 *K–M*).

Discussions

Our study confirmed several predictions of previous investigators discussed above about the mechanism of autoactivation and autorepression of P_{RM} by measuring in vitro transcription on supercoiled DNA templates containing different combinations of operator mutations. Our transcription data support the model that autoactivation requires CI binding to O_R2, and that activation is stimulated by cooperative dimer–dimer and tetramer–tetramer interactions between CI molecules at O_R2 and those bound to other operator subsites. First, cooperative interactions of CI not only occur between O_R1 and O_R2 *in cis*, as reported previously, but also between $O_R1 \sim O_R2$ and $O_L1 \sim O_L2$ *in trans*, resulting in individual site occupancies at lower CI concentrations as judged by their effects on P_{RM} activation. The *trans*-cooperativity by octamer formation requires adjacent CI binding sites between $O_R1 \sim O_R2/O_L1 \sim O_L2$ or $O_R1 \sim O_R2/O_L2 \sim O_L3$ and not $O_R1 \sim O_R2$ and $O_L1 \sim O_L3$ (Fig. S3 *F* and *J*). Similar *trans*-cooperativity between O_R3 and O_L3 is inferred from P_{RM} repression at lower CI concentrations. Cooperative interactions lead to DNA looping when they occur between CI at O_L and O_R sites. P_{RM} is autorepressed by the binding of CI to O_R3 as reported previously (1–3), and this is stimulated by dimer–dimer and tetramer–tetramer interactions that occur through DNA looping. Our results are in agreement with Revet et al. (18) that looping per se strengthens the binding of CI to the suboperators (Fig. 5). Our work provided quantitative evaluation of the contribution of each operator to autoregulation.

Autoactivation. Given that the presence of O_L promotes DNA looping, we demonstrated in vitro that looping further enhances activation. In vivo, a twofold activation of P_{RM} by an octameric loop was observed by Anderson and Yang (27, 28), although Little and Michalowski showed a substantial increase (*ca.* fivefold) in P_{RM} by looping on *prm*240, a weak P_{RM} variant (41). To characterize the conditions that affect activation, the O_R3 site was mutated to alleviate repression of $P_{RM}1$. Comparison of the $O_L3^- O_R3^-$ and the $O_L^- O_R3^-$ templates revealed that looping enhances the activation of $P_{RM}1$ by 1.6-fold at maximum activation levels. The mechanism of enhancement of P_{RM} activation by an octameric DNA loop formation may simply be by the associated tighter binding of CI to O_R2.

Autorepression. We showed that, in a template with WT operators and promoters, the repression of P_{RM} commenced above 80 nM CI and was almost fully repressed above 400 nM. The physiological concentration of monomeric CI in a lysogenic cell was estimated to be approximately 200 nM (6, 17, 30, 31). Therefore, in our system, repression of P_{RM} was observed above physiological conditions. When we tested the regulation of $P_{RM}1$ by CI, only partial repression of $P_{RM}1$ occurred in the absence of O_L, even at 1,600 nM CI, implying that the binding of CI to O_R3 is not sufficient for complete repression of $P_{RM}1$. However, when O_L was present, complete repression was observed, confirming that autorepression requires DNA looping, as was suggested from in vivo experiments (19). It has been proposed that an interaction between CI dimers at O_L3 and one at O_R3 helps CI binding to the latter, but only when looping has occurred with CI bound to $O_L1 \sim O_L2$ and $O_R1 \sim O_R2$ (19). CI has higher affinity for O_L3 than for O_R3 (11, 13, 15, 53). Our in vitro transcription experiments using various combinations of O_L mutants confirmed the involvement of O_L3 in P_{RM} repression but also showed the involvement of O_L2 in efficient O_R3 mediated $P_{RM}1$ repression by CI. In O_R^+ templates, the presence of an O_L3^- or O_L2^-, but not O_L1^- mutation failed to show P_{RM} repression at lower CI concentration (Fig. 4 *C–E* and Fig. S3 *A–D*). The results further suggest that the cooperative help of CI from O_L3 to CI at O_R3 can only occur if CI also binds to the adjacent element O_L2. Note that (*i*) the involvement of the O_L element toward P_{RM} repression is indirect and through O_R, (*ii*) DNA looping can occur by octamer formation at $O_L1 \sim O_L2$ and $O_R1 \sim O_R2$ or $O_L2 \sim O_L3$ and $O_R1 \sim O_R2$.

In summary, our results confirm that DNA loops in prophage λ are likely to contain, in the absence of mutations, four CI dimers (two CI at $O_R1 \sim O_R2$ and two at $O_L1 \sim O_L2$ forming an octamer) or six CI dimers (an additional dimer pair connecting O_R3 and O_L3). The octamer-mediated loop is less stable on linear DNA (25). We show that looping enhances autoactivation of $P_{RM}1$ as long as O_R3 does not become occupied. We confirmed that the loop that enhances the autoactivation is the octamer-mediated, thermodynamically less-stable loop. We also show that, at physiological CI concentrations, looping is essential for P_{RM} repression but only the stable octamer plus tetramer-mediated form can do so.

Transcription of the *cI* gene from the P_{RM} promoter in a lysogen occurs at multiple levels: (*i*) basal transcription; (*ii*) activated transcription by CI without any DNA loop; (*iii*) enhanced activated transcription by a loop comprising four CI dimers; and (*iv*) repression of basal transcription by a loop containing six CI dimers. This polymorphic behavior of P_{RM} regulations by a single protein enables the lysogen to maintain a steady but very low level of free CI in a λ lysogen. This low level may allow fast degradation of free CI by SOS, which is induced by RecA, a coprotease (54, 55), and thus easy switching of the prophage to a lytic state. It is interesting to notice that the maintenance of a biologically critical level of CI involves formation and interconversion of two topographically different forms of a loop.

Materials and Methods

Proteins. *E. coli* RNA polymerase (1 unit/μL) was from USB/Affymetrix. WT CI and mutant (G147D, D197G) proteins were purchased from Protein RST. They were more than 98% pure as estimated by Coomassie staining of SDS gels. Modified Lowry Protein Assay was used to determine the total CI monomer concentrations.

Plasmid Constructions. Details of plasmid constructions are given in the *SI Text*. The plasmids used in this study are listed in Table S1. Table S2 contains the primers used in the construction of WT plasmid pDL944 as described in Fig. S6.

In Vitro Transcription Assays. In vitro transcription reactions were performed as described (56). Bacteriophage λ repressor CI (20–1,600 nM) was added to supercoiled DNA templates (4 nM) and the different promoters were transcribed by 20 nM RNA polymerase in the presence of nucleoside 5'-triphosphates and 5 μCi [α-^{32}P]UTP (1Ci = 37 GBq) (3,000 Ci/mmol). The RNAI transcripts present in the plasmids (106 and 108 nts) were used as internal controls to quantify the relative amount of transcripts from P_R, P_L, and P_{RM} (57). The relative amount of transcripts in the presence of CI was normalized to that in the absence of CI. P_{RM} transcripts migrated as 212 nt, P_L as 167 nt and P_R as 117 nt on templates where O_R3 is separated from O_L3 by 392 bp. In vitro, we observed two rounds of transcription in our assays (58). Details of in vitro transcription assay are described in the *SI Text*.

ACKNOWLEDGMENTS. We thank Donald Court and Robert Weisberg for helpful discussions. We especially thank Gary Gussin, Jeffrey Roberts, Ann Hochschild, and John Little for critical comments on the manuscript. This work was supported by the Intramural Research Program of the National Institutes of Health, the National Cancer Institute, the Center for Cancer Research, and by an Extramural Research Grant, RGM084070A.

1. Meyer BJ, Maurer R, Ptashne M (1980) Gene regulation at the right operator (OR) of bacteriophage lambda. II. OR1, OR2, and OR3: Their roles in mediating the effects of repressor and cro. *J Mol Biol* 139:163–194.

2. Meyer BJ, Ptashne M (1980) Gene regulation at the right operator (OR) of bacteriophage lambda. III. lambda repressor directly activates gene transcription. *J Mol Biol* 139:195–205.

3. Maurer R, Meyer B, Ptashne M (1980) Gene regulation at the right operator (OR) bacteriophage lambda. I. OR3 and autogenous negative control by repressor. *J Mol Biol* 139:147–161.
4. Yen KM, Gussin GN (1973) Genetic characterization of a prm- mutant of bacteriophage lambda. *Virology* 56:300–312.
5. Eisen H, Brachet P, Pereira da Silva L, Jacob F (1970) Regulation of repressor expression in lambda. *Proc Natl Acad Sci USA* 66:855–862.
6. Reichardt L, Kaiser AD (1971) Control of lambda repressor synthesis. *Proc Natl Acad Sci USA* 68:2185–2189.
7. Ptashne M (2004) *A Genetic Switch: Phage Lamba Revisited* (Cold Spring Harbor Laboratory Press, Plainview, New York), 3rd Ed.
8. Meyer BJ, Kleid DG, Ptashne M (1975) Lambda repressor turns off transcription of its own gene. *Proc Natl Acad Sci USA* 72:4785–4789.
9. Ptashne M, et al. (1976) Autoregulation and function of a repressor in bacteriophage lambda. *Science* 194:156–161.
10. Ptashne M, et al. (1980) How the lambda repressor and cro work. *Cell* 19:1–11.
11. Takeda Y, Sarai A, Rivera VM (1989) Analysis of the sequence-specific interactions between Cro repressor and operator DNA by systematic base substitution experiments. *Proc Natl Acad Sci USA* 86:439–443.
12. Sarai A, Takeda Y (1989) Lambda repressor recognizes the approximately 2-fold symmetric half-operator sequences asymmetrically. *Proc Natl Acad Sci USA* 86:6513–6517.
13. Shea MA, Ackers GK (1985) The OR control system of bacteriophage lambda. A physical-chemical model for gene regulation. *J Mol Biol* 181:211–230.
14. Ackers GK, Shea MA, Smith FR (1983) Free energy coupling within macromolecules. The chemical work of ligand binding at the individual sites in co-operative systems. *J Mol Biol* 170:223–242.
15. Koblan KS, Ackers GK (1992) Site-specific enthalpic regulation of DNA transcription at bacteriophage lambda OR. *Biochemistry* 31:57–65.
16. Johnson AD, Meyer BJ, Ptashne M (1979) Interactions between DNA-bound repressors govern regulation by the lambda phage repressor. *Proc Natl Acad Sci USA* 76:5061–5065.
17. Ackers GK, Johnson AD, Shea MA (1982) Quantitative model for gene regulation by lambda phage repressor. *Proc Natl Acad Sci USA* 79:1129–1133.
18. Revet B, von Wilcken-Bergmann B, Bessert H, Barker A, Muller-Hill B (1999) Four dimers of lambda repressor bound to two suitably spaced pairs of lambda operators form octamers and DNA loops over large distances. *Curr Biol* 9:151–154.
19. Dodd IB, Perkins AJ, Tsemitsidis D, Egan JB (2001) Octamerization of lambda CI repressor is needed for effective repression of P(RM) and efficient switching from lysogeny. *Genes Dev* 15:3013–3022.
20. Dodd IB, et al. (2004) Cooperativity in long-range gene regulation by the lambda CI repressor. *Genes Dev* 18:344–354.
21. Svenningsen SL, Costantino N, Court DL, Adhya S (2005) On the role of Cro in lambda prophage induction. *Proc Natl Acad Sci USA* 102:4465–4469.
22. Wang H, Finzi L, Lewis DE, Dunlap D (2009) AFM studies of lambda repressor oligomers securing DNA loops. *Curr Pharm Biotechnol* 10:494–501.
23. Griffith J, Hochschild A, Ptashne M (1986) DNA loops induced by cooperative binding of lambda repressor. *Nature* 322:750–752.
24. Hochschild A, Ptashne M (1986) Cooperative binding of lambda repressors to sites separated by integral turns of the DNA helix. *Cell* 44:681–687.
25. Zurla C, et al. (2009) Direct demonstration and quantification of long-range DNA looping by the lambda bacteriophage repressor. *Nucleic Acids Res* 37:2789–2795.
26. Zurla CFA, et al. (2006) Novel tethered particle motion analysis of CI protein-mediated DNA looping in the regulation of bacteriophage lambda. *J Phys Condens Matter* 18: S225–S234.
27. Anderson LM, Yang H (2008) A simplified model for lysogenic regulation through DNA looping. *Conf Proc IEEE Eng Med Biol Soc* 2008:607–610.
28. Anderson LM, Yang H (2008) DNA looping can enhance lysogenic CI transcription in phage lambda. *Proc Natl Acad Sci USA* 105:5827–5832.
29. Huang J, Schlick T, Vologodskii A (2001) Dynamics of site juxtaposition in supercoiled DNA. *Proc Natl Acad Sci USA* 98:968–973.
30. Pirrotta V, Chadwick P, Ptashne M (1970) Active form of two coliphage repressors. *Nature* 227:41–44.
31. Johnson AD, et al. (1981) lambda Repressor and cro-components of an efficient molecular switch. *Nature* 294:217–223.
32. Guarente L, Nye JS, Hochschild A, Ptashne M (1982) Mutant lambda phage repressor with a specific defect in its positive control function. *Proc Natl Acad Sci USA* 79:2236–2239.
33. Hwang JJ, Brown S, Gussin GN (1988) Characterization of a doubly mutant derivative of the lambda PRM promoter. Effects of mutations on activation of PRM. *J Mol Biol* 200:695–708.
34. Virnik K, et al. (2003) "Antiparallel" DNA loop in gal repressosome visualized by atomic force microscopy. *J Mol Biol* 334:53–63.
35. Geanacopoulos M, Vasmatzis G, Zhurkin VB, Adhya S (2001) Gal repressosome contains an antiparallel DNA loop. *Nat Struct Biol* 8:432–436.
36. Humayun Z, Kleid D, Ptashne M (1977) Sites of contact between lambda operators and lambda repressor. *Nucleic Acids Res* 4:1595–1607.
37. Jain D, Nickels BE, Sun L, Hochschild A, Darst SA (2004) Structure of a ternary transcription activation complex. *Mol Cell* 13:45–53.
38. Albright RA, Matthews BW (1998) How Cro and lambda-repressor distinguish between operators: The structural basis underlying a genetic switch. *Proc Natl Acad Sci USA* 95:3431–3436.
39. Beamer LJ, Pabo CO Refined 1.8 A crystal structure of the lambda repressor-operator complex. *J Mol Biol* 227:177–196.
40. Jordan SR, Pabo CO (1988) Structure of the lambda complex at 2.5 A resolution: Details of the repressor-operator interactions. *Science* 242:893–899.
41. Little JW, Michalowski CB (2010) Stability and instability in the lysogenic state of phage lambda. *J Bacteriol* 192:6064–6076.
42. Giladi H, Murakami K, Ishihama A, Oppenheim AB (1996) Identification of an UP element within the IHF binding site at the PL1–PL2 tandem promoter of bacteriophage lambda. *J Mol Biol* 260:484–491.
43. Giladi H, Koby S, Gottesman ME, Oppenheim AB (1992) Supercoiling, integration host factor, and a dual promoter system, participate in the control of the bacteriophage lambda pL promoter. *J Mol Biol* 224:937–948.
44. Burz DS, Beckett D, Benson N, Ackers GK (1994) Self-assembly of bacteriophage lambda cI repressor: Effects of single-site mutations on the monomer-dimer equilibrium. *Biochemistry* 33:8399–8405.
45. Beckett D, Burz DS, Ackers GK, Sauer RT (1993) Isolation of lambda repressor mutants with defects in cooperative operator binding. *Biochemistry* 32:9073–9079.
46. Whipple FW, Kuldell NH, Cheatham LA, Hochschild A (1994) Specificity determinants for the interaction of lambda repressor and P22 repressor dimers. *Genes Dev* 8:1212–1223.
47. Burz DS, Ackers GK (1994) Single-site mutations in the C-terminal domain of bacteriophage lambda cI repressor alter cooperative interactions between dimers adjacently bound to OR. *Biochemistry* 33:8406–8416.
48. Bell CE, Frescura P, Hochschild A, Lewis M (2000) Crystal structure of the lambda repressor C-terminal domain provides a model for cooperative operator binding. *Cell* 101:801–811.
49. Dove SL, Joung JK, Hochschild A (1997) Activation of prokaryotic transcription through arbitrary protein-protein contacts. *Nature* 386:627–630.
50. Whipple FW, Hou EF, Hochschild A (1998) Amino acid-amino acid contacts at the cooperativity interface of the bacteriophage lambda and P22 repressors. *Genes Dev* 12:2791–2802.
51. Jana NK, Roy S, Bhattacharyya B, Mandal NC (1999) Amino acid changes in the repressor of bacteriophage lambda due to temperature-sensitive mutations in its cI gene and the structure of a highly temperature-sensitive mutant repressor. *Protein Eng* 12:225–233.
52. Stayrook S, Jaru-Ampornpan P, Ni J, Hochschild A, Lewis M (2008) Crystal structure of the lambda repressor and a model for pairwise cooperative operator binding. *Nature* 452:1022–1025.
53. Sarai A (1989) Molecular recognition and information gain. *J Theor Biol* 140:137–143.
54. Little JW (1984) Autodigestion of lexA and phage lambda repressors. *Proc Natl Acad Sci USA* 81:1375–1379.
55. Little JW, Mount DW (1982) The SOS regulatory system of Escherichia coli. *Cell* 29:11–22.
56. Lewis DE (2003) Identification of promoters of Escherichia coli and phage in transcription section plasmid pSA850. *Methods Enzymol* 370:618–645.
57. Tomizawa J, Itoh T, Selzer G, Som T (1981) Inhibition of ColE1 RNA primer formation by a plasmid-specified small RNA. *Proc Natl Acad Sci USA* 78:1421–1425.
58. Lewis DE, Komissarova N, Le P, Kashlev M, Adhya S (2008) DNA sequences in gal operon override transcription elongation blocks. *J Mol Biol* 382:843–858.
59. Hochschild A (2002) The lambda switch: cI closes the gap in autoregulation. *Curr Biol* 12:R87–89.